Article

J. Mex. Chem. Soc. **2008**, *52(3),* 201-211

ISSN 1870-249X

Structure-activity of Sansalvamide A Derivatives and their Apoptotic Activity in the Pancreatic Cancer Cell Line PL-45

Rodrigo A. Rodríguez, Po-Shen Pan, Robert C. Vasko, Chung-Mao Pan, William S. Disman, Shelli R. McAlpine*

Department of Chemistry and Biochemistry, San Diego State University, 5500 Campanile Drive, San Diego, CA 92182-1030

Recibido el 1 de mayo de 2008; aceptado el 7 de julio de 2008

Abstract: We report the structure-activity relationship (SAR) of forty Sansalvamide A (San A) derivatives against human pancreatic ductal adenicarcinoma cell line PL-45. Our comprehensive evaluation of these compounds utilizes: cytotoxicity based SAR, molecular modeling, and ApoAlert Annexin V apoptosis detection to evaluate these potent compounds. Compared to current pancreatic cancer drugs, these San A analogs are structurally unique, and are potentially cytotoxic. Our comprehensive studies including molecular modeling show that a single *N*-methyl, a single *D*-amino acid (*D*-aa) or a single N -methyl *D*-aa appears to be critical for presenting the active conformation of San A peptide derivates to its biological target, and show that the San A peptide derivative **8** has the ability to selectively induce apoptosis. Thus, showing that this class of compounds are promising chemotherapeutic agents that will eliminate cells in an orderly manner without eliciting an undesired immune response.
Key words: structure-activity relationship, Sansalvamide A, human pancreatic adenicarcinoma, molecular modeling, apoptosis.

Resumen: Se describe la relación estructura-actividad (REA) de cuarenta derivados de Sansalvamida A (San A) frente a la línea celular PL-45 de adenocarcinoma ductal de páncreas humano. Para la evaluación de estos compuestos se hizo uso de: determinación de la citotoxicidad basada en REA, modelado molecular y detección de apoptosis ApoAlert Annexina V. Comparados a los medicamentos actualmente en uso contra cáncer pancreático, estos análogos de San A de estructura novedosa presentaron actividad citotóxica importante. Nuestros estudios que incluyen modelado molecular muestran que ya sea un solo grupo *N*-metilo, o un *D*-aminoácido (*D*-aa) o un *N*-metil *D*-aa pueden ser críticos para presentar la conformación activa del derivado peptídico de San A en su blanco biológico; además muestran que el derivado **8** tiene la habilidad de inducir selectivamente apoptosis. De esta forma, se muestra que esta clase de compuestos son agentes quimioterapéuticos prometedores que eliminan células de manera ordenada, sin presentar una respuesta inmune indeseable.
Palabras clave: relación estructura-actividad, Sansalvamida A, adenocarcinoma de páncreas humano, modelado molecular, apoptosis.

Introduction

Pancreatic cancer is the fifth most deadly cancer in the U.S. Less than 20% of pancreatic cancers respond to the drug of choice [2,2-difluorodeoxycytidine] or other drugs on the market. Only 10% of patients are eligible for surgery, and the five-year mortality rate for patients diagnosed with pancreatic cancers is 95% [1]. Such low response rates to current chemotherapeutic treatments demands an immediate need for new drugs that provide additional chemotherapeutic options to patients.

The Sansalvamide A (San A) natural product was isolated in 1999 by Fenical and co-workers from a marine fungus (Fusarium sp.) and exhibits anti-tumor activity [2,3]. San A natural product is a depsipeptide with a lactone at position 4 (**Figure 1**). In attempts to avoid deactivation by ring opening esterases, all San A derivatives reported here were synthesized as the San A peptide derivatives (**Figure 1**, amino acid 4). Cytotoxicity of the San A natural product and its derivatives against pancreatic [4-6], colon [3,7-10], breast, prostate, and melanoma cancers [4] clearly indicate the San A derivatives potential as new therapeutic agents for the treatment of various cancers and support further exploration of this class of compounds. Further one hallmark of cancer is the deregulation of the natural process of apoptosis, which leads to the overproduction of cells causing tumor formation [11]. Thus, one essential mechanism of action against cancer is the selective restoration of the natural apoptotic process so that carcinogenetic cells may enter into an organized mechanism of death. Analogs of San A have been found to induce G0/G1 phase cell-cycle arrest and induce apoptosis in two human pancreatic cell lines (AsPC-1 and S2-01) [5]. It is important to note that these apoptosis detection studies were performed using serum-deprived cells. It is also well known that depriving factor-dependent cells of colony-stimulating factors such as serum will by itself lead to apoptosis [12]. Thus, in this manuscript we demonstrate that our compounds induce apoptosis under non-serum deprived conditions.

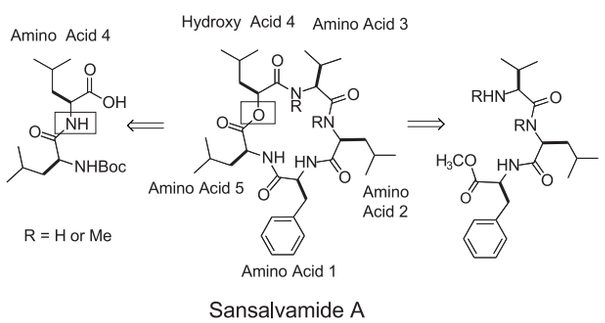

Fig. 1. Retrosynthetic Strategy.

Results and Discussion

Herein we describe a comprehensive evaluation of forty San A peptide derivatives utilizing key SAR derived from cytotoxic ^{3}H-thymidine inhibition data, molecular modeling, as well as an Annexin V apoptosis detection study. The compounds studied generally follow the rules set by Lipinski regarding oral availability of a drug, including no more than five H-doners, no more than 10 H-acceptors, molecular weights ranging from 500-600, and logP values ≤ 5.0 [13]. Although some of the more active San A derivatives are just outside of these ranges (MW's of 550-640 and ClogPs ranging from 5-7) Given that our derivatives share no homology with other classes of chemotherapeutic agents and they are as potent as current drugs on the market, we feel that this class of compounds exhibits potential structures for further chemotherapeutic development. Our extensive SAR studies described here show that San *A*-peptides cytotoxicity in PL-45 is due to the placement of a single *D* or single *N*-methyl or single *N*-methyl-*D*-aa. Although having one of these three features does not guarantee a potent compound, it seems to be a criterion that is required for any compound to prove successfully potent. This observed SAR is validated by several examples in the recent literature where cyclic peptides, specifically pentapeptides with a single *D*-aa, lock the macrocycle into a single conformation [14,15]. Our molecular modeling studies tested two analogs (**8** and **9**) against PL-45, and through conformational searches we have obtained an optimal structure from the lowest energy diagrams using the MMFF94 force field. In order to evaluate the mode of action for these compounds, San A derivative **8** was tested for its ability to induce apoptosis in PL-45 pancreatic cancer cells using flow cytometry and Annexin V protein-FITC chromophore conjugates and non-serum deprived cells. These non-serum deprived assays definitively show that compound **8** causes cell death in pancreatic cancer cells through the apoptosis pathway, where selective apoptotic inducers are highly sought after because they eliminate cells in an orderly manner without eliciting an undesired immune response.

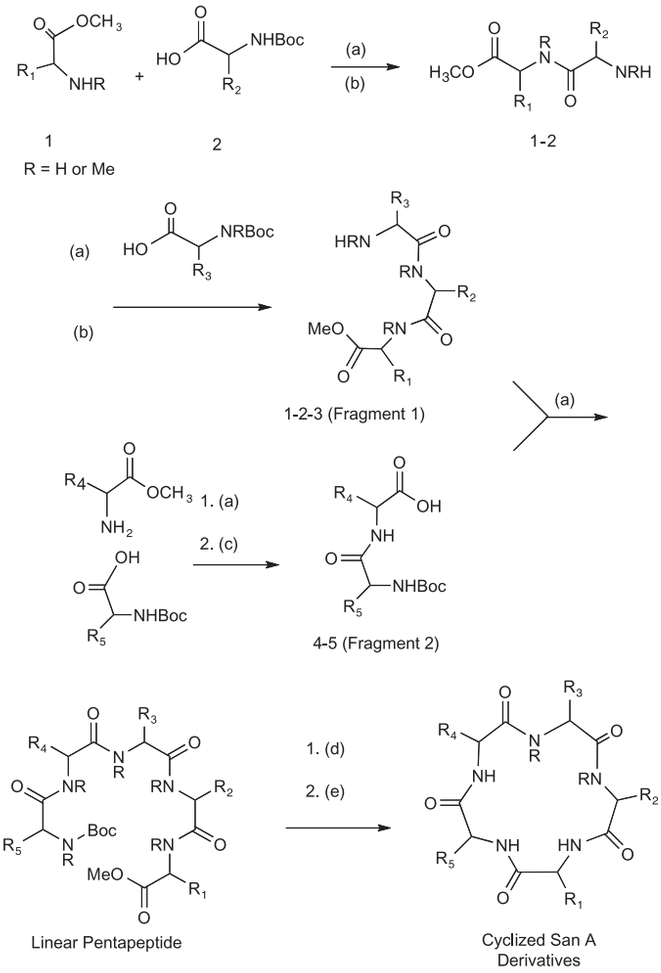

Fig. 2. Synthesis of Macrocycles Conditions: a) coupling agent, DIPEA (3 equiv), CH_2Cl_2 (0.1*M*), b)TFA (20%), Anisole (2 equiv), CH_2Cl_2, c) LiOH (4 equiv), MeOH d) HCl in THF (0.05*M*), Anisole (2 equiv), e) HATU (0.7 equiv), DEPBT (0.7 equiv), TBTU (0.7 equiv), DIPEA (6 equiv), THF:CH_3CN:CH_2Cl_2 (2:2:1) 0.007*M*. TBTU (1.2 equiv), and/or HATU (0.75 equiv)[18] .

Synthetic Strategy

Described here is our synthetic approach for the synthesis of forty San *A* peptide derivatives which utilized a convergent solution-phase approach (Figure 1) [8,16]. This strategy is a reliable and inexpensive route which provides access to the synthesis of gram quantities of these compounds required for additional biological studies (Figure 2). The described compounds provide valuable information with regards to stereochemistry, *N*-methyl moieties, amide bond geometry, hydrophobic, hydrophilic, and aliphatic effects on potency.

Synthesis

The synthesis of the San *A* derivatives were completed using the amino acids shown in **Figure 3** via a synthetic strategy shown (**Figure 2**). These forty compounds have been generated over two generations (structures shown in **Figures 4-9**), with the most potent compounds almost exclusively coming from the second-generation [10]. Thus, we demonstrate the ability to incorporate potent features into our progressive design. Using 2(1-H-benzotriazole-1-yl)-1,1,3-tetramethyluronium tetrafluoroborate (TBTU), and diisopropylethylamine (DIPEA), acid protected residue **1a-e** and N-Boc protected residue **2a-h** were coupled to give the dipeptide 1-2-Boc (80-94% yield). Deprotection of the amine on residue **2** using TFA gave the free amine, **1-2** (~quantitative yields). Coupling of the dipeptide to monomer **3a-g** gave the desired tripeptide (Fragment 1) in good yields (80%-95%) [17]. The synthesis of Fragment 2 was completed by coupling residue **4**a-e to residue **5**a-f to give dipeptide **4-5**-Boc (90-95% yield). The amine was deprotected on Fragment 1 using TFA and the acid was revealed in Fragment 2 using lithium hydroxide. Fragment 1

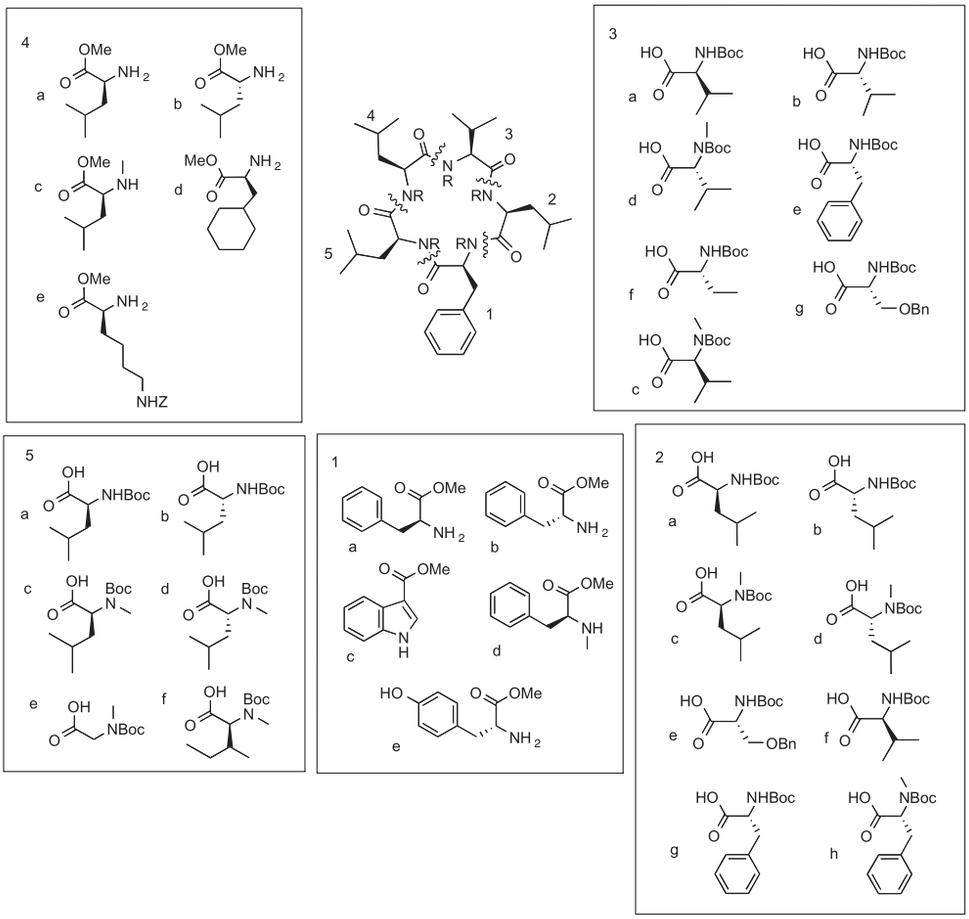

Fig. 3. Amino acids used in the synthesis of forty derivatives.

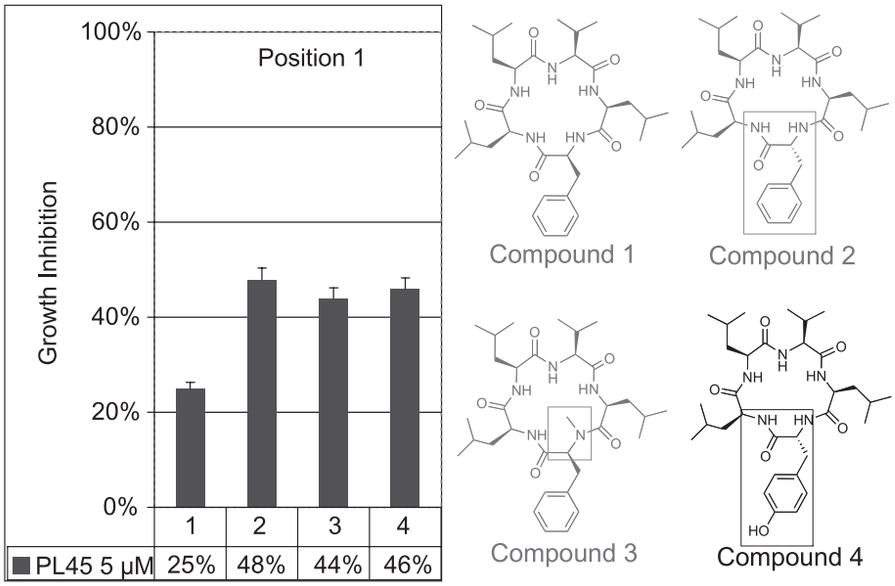

Fig- 4: Compounds with changes to position 1. Grey compounds **1**, **2**, and **3** are first generation compounds, while black compound **4**, is second-generation. Each data point is an average of three wells run in three assays. Error = ±5%.

and Fragment 2 were coupled using multiple coupling agents [9,18,19], yielding linear pentapeptides (66-90% yield) [17]. In the case of the di- and tripeptide construction, acid/base workup removed excess reagents and side products, and the NMR indicated compounds did not require further purification. Only in the case of pentapeptides and macrocycles did we find it necessary to purify compounds via silica chromotography, making the synthesis efficient. The purity of all compounds was verified via NMR and/or LCMS. The linear peptides were then cyclized using conditions developed in our laboratory [16]. Upon cyclization, the final compounds were purified via flash chromotography and/or HPLC. When appropriate, the side chains were deprotected (serines, lysines, and tyrosines). The purity of all compounds was verified by NMR and LCMS [16].

Structure-activity relationships (SAR)

Forty San A analogs have been tested for cytotoxicity against human pancreatic ductal adenicarcinoma cell line PL-45. Potency exhibited by the San *A* peptide (**1**) is shown so that comparisons can be made between the natural product peptide and our synthetic analogs. The histograms in Figures 4-8 show the percent growth inhibition produced by a concentration of 5 μM compound in the PL-45 cell line with changes at positions 1-5 respectively. Compounds **2** and **3** are first generation compounds (grey, Figure 4), while **4** is second-generation (black). Changes involved the incorporation of a single D-aa in position 1, **2** and **4**, or an *N*-methyl at position 1, compound **3**. Both changes to the configuration at this position produced compounds that are more potent than compound **1**, suggesting that there is a conformational element that is key to the potency of these compounds. These two compounds displayed ~2 fold improved growth inhibition over the natural product peptide **1**.

The histogram in Figure 5 shows the growth inhibition of compounds with changes to the configuration at position 2. Compounds **5**, **6**, and **7** are first generation compounds (grey, Figure 5), while **8**, **9**, and **10** are second-generation compounds (black). The first generation compounds involved incorporation of an *N*-methyl in position 2 (compound **5**), or a *D*-aa, compound **6**, or both features, compound **7**. First generation compounds **5** and **6** demonstrate some improved potency over that seen with **1**, indicating that including a single *N*-methyl or a D-aa do improve cytotoxicity against this cell line. Interestingly, incorporating both features does not provide a potent compound i.e. **7**. The second-generation compounds include compound **8**, which shows excellent cytotoxicity against PL-45 (70% inhibition), where this compound is similar to **7** as it contains both an *N*-methyl and *D*-aa, but unlike **7**, it contains an *N*-methyl D-phe in place of leucine. Interestingly, **9**, which only differs from **8** by an *N*-methyl, has a significantly lower potency. In summary, an *N*-methyl-leu or *D*-leu generate compounds with improved effectiveness, but the combination is not effective. However, an *N*-methyl *D*-phe combination generates the most toxic compound in this series. These conclusions suggest that there is not only a positional effect but there is also a conformational requirement that is key to potency.

Compounds **11**, **12**, **13**, and **14** are first generation compounds (grey, Figure 6), while compounds **15**, **16**, **17**, and **18** are second-generation (black). The first generation compounds involved incorporation of an *N*-methyl in position 3 (**11**), or a D-aa (**12**), or both (**14**), where placement of a single D-valine at position 3 (**12**) produced an extraordinarily potent compound against PL-45 cell line. Yet, an *N*-methyl or an *N*-methyl-D-valine at position 3 generates a non-potent compound, compounds **11** and **14,** respectively. Further, a *D*-valine combined with other alterations, i.e. compounds **13**, **18**, **22**, **23**, **24**, **38**, **39**, and **40** all show much lower potency than **12**. This strongly indicates that there is a specific role played by a single *D*-valine at 3 that places the ring into an appropriate conformation for binding to its target and inducing a cytotoxic effect. Interestingly, placement of an *N*-methyl-*D*-valine at 3, combined with a hydrophobic cyclohexyl at 4, generates the relatively potent compound **22** (Figure 7), and the incorporation of a polar (**15**), or hydrophobic aromatic (**16**), or ethyl (**17**) element at position 3, all diminish the compounds' activity relative to San *A* peptide (**1**).

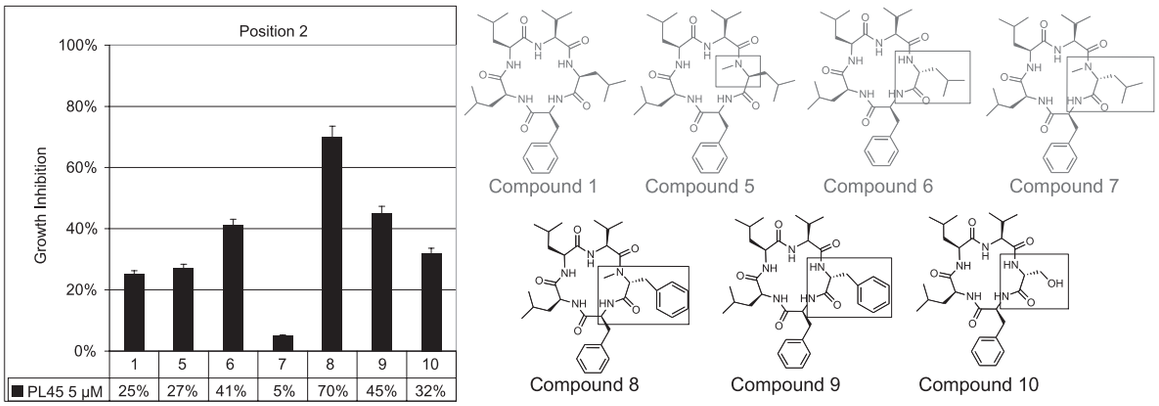

Fig. 5. Compounds with changes to position 2. Grey compounds **5**, **6**, and **7** are first generation compounds, while black compounds **8**, **9**, and **10**, are second-generation. Each data point is an average of three wells run in three assays Error = ±5%.

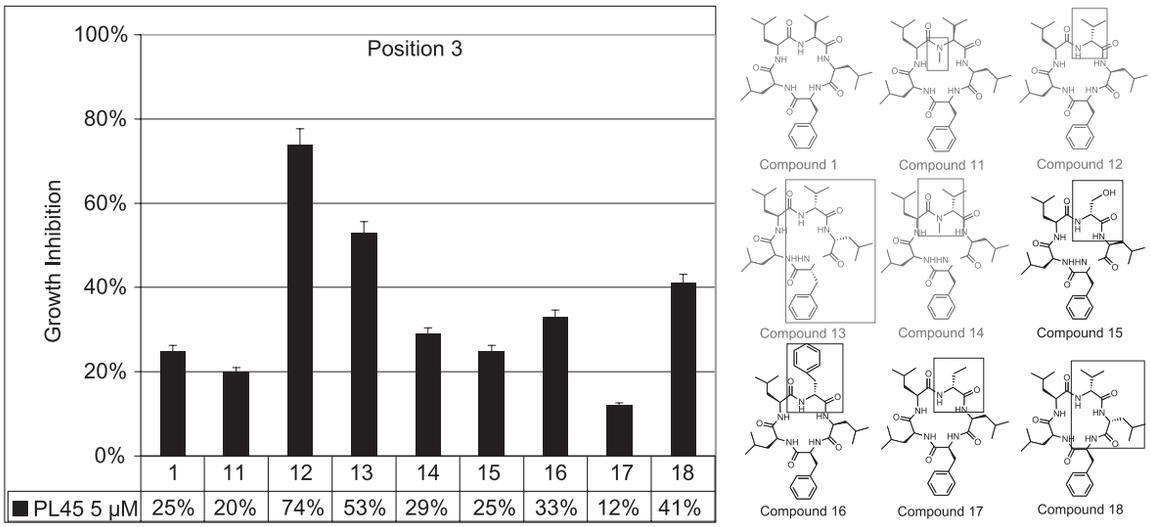

Fig. 6. Compounds with changes to position 3. Grey compounds **11**, **12**, **13**, and **14** are first generation compounds, while black compounds **15**, **16**, **17**, and **18** are second-generation. Each data point is an average of three wells run in three assays. Error = ±5%.

Compounds **19** and **20** are first generation compounds (grey, Figure 7), while compounds **21**, **22**, **23**, **25**, **27**, **24**, **26**, and **28** are second-generation (black). The first generation compounds involved incorporation of a *D*-aa (**19**), or *N*-methyl at 4 (**20**). In addition, an *N*-methyl at 4 and a *D*-aa at 5 generated (**38**), and two *D*-aa's in positions 4 and 5 provided (**35**). Unlike in position 3, e.g. compound **12**, it seems that the placement of a single *D*-aa in position 4 does not provide a compound with potency against PL-45, but rather placement of a single *D*-aa in position 4 renders inactive compound **19**. Interestingly, a single *N*-methyl at 4, or the combination of an *N*-methyl at 4 and *D*-aas at 1 and 5, provides the fifth most potent compound in this series: **34** (Figure 8). In summary, these data also suggest that conformational control is being excerpted over the compounds via the inclusion of an *N*-methyl, *D*-aa or a combination of these structural elements. Furthermore, evidence of polar groups decreasing potency can be observed by the difference between compounds **24** and **23** at position 4, where the only change is the removal of a benzyl carbamate (Cbz) group. The increased polarity of the free lysine side chain in compound **23** results in decreased potency compared to its Cbz protected counter part **24**.

Compounds **29**, **30**, **31**, **32**, and **33** are first generation compounds with substitutions focusing on position 5, (grey, Figure 8), while compounds **34**, **35**, **36**, **37**, **38**, **39**, and **40** are second-generation (black). The first generation compounds involved incorporation of an *N*-methyl (**30**) or a *D*-aa at 5 (**32**). These two compounds showed growth inhibition at ≥ 44% for PL-45. Compound **30** led to the exploration of *N*-methyl moieties at position 5. From the SAR, it seems the that placement of a single *N*-methyl is not generally favorable for potency enhancement unless it is placed in a key position i.e. position 5. Thus, incorporating a single *N*-methyl moiety to the San *A* cyclic peptide is best done at position 5. This conclusion is supported by the fact that compounds with *N*-methyls at positions 2 or 3 are not active (compounds **3** and **11**, respectively) and the incorporation at positions 1 or 4 gives less active compounds, **3** and **20** respectively, compared to compounds with an *N*-methyl at 5 i.e. compounds **36** and **37**. It is interesting to note that compound **30** shows similar growth inhibition to its enantiomer **31**. Also, the combination of a *D*-valine in position 3, with an *N*-methyl glycine at position 5 produced **36,** the most potent compound in this entire series. However, inclusion of an *N*-methyl moiety is not the only key element in controlling potency for this class of compounds. This can be clearly observed by comparing the activities of compounds **33** and **34**, where the only difference between these two compounds is that **34** contains a *D*-aa at position 1. Yet, compound **34** displays a 2.4 fold higher growth inhibition than **33**.

Finally, a single change in the configuration at position 5 to a *D*-aa provides compound **32**, which has potency on par with that of **12**. As mentioned earlier, compound **12** only differs by a single D-aa change to position 3 compared to the San A natural product and interestingly it is the second most potent compound in the PL-45 series. Compounds **12** and now **32** provide further evidence that the placement of a single D-aa in a key position may give rise to the making of a highly active compound against PL-45 [6].

Summary of SAR results

After testing forty compounds we have identified several important factors contributing to potency in the PL-45 cell line. An important feature is the inclusion of an *N*-methyl next to two adjacent *D*-aa's (**34**). Previous studies have shown that a single *N*-methyl *D*-aa is needed to lock the macrocycle into its lowest energy conformation, and **34** proves to be an expan-

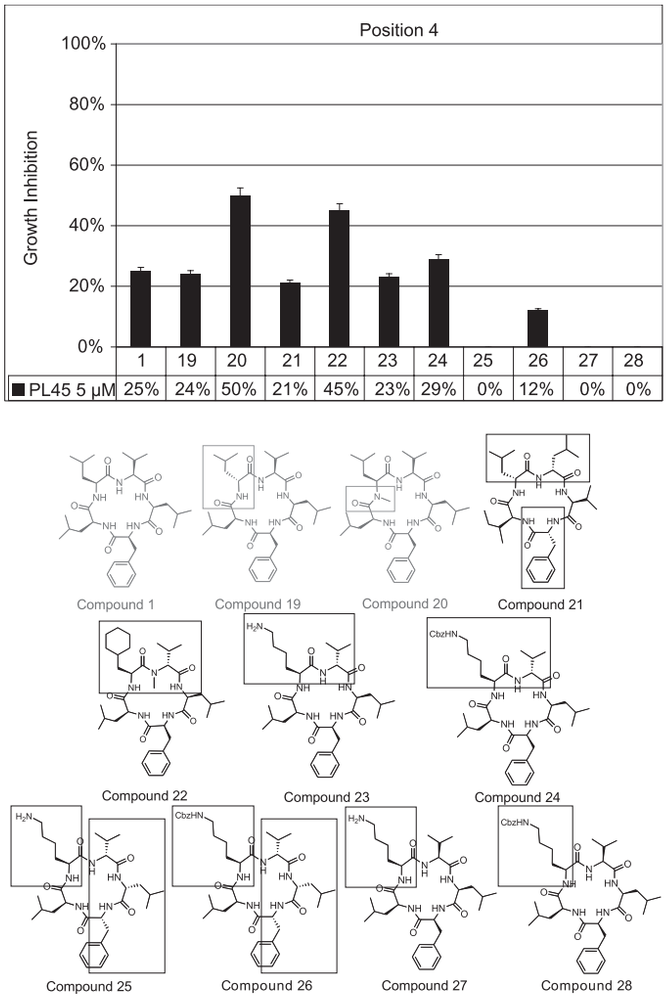

Fig. 7. Compounds with changes to position 4. Grey compounds **19**, and **20** are first generation compounds, while black compounds **21**, **22**, **23**, **24**, **25**, **26**, **27**, and **28** are second-generation. Each data point is an average of three wells run in three assays. Error = ±5%.

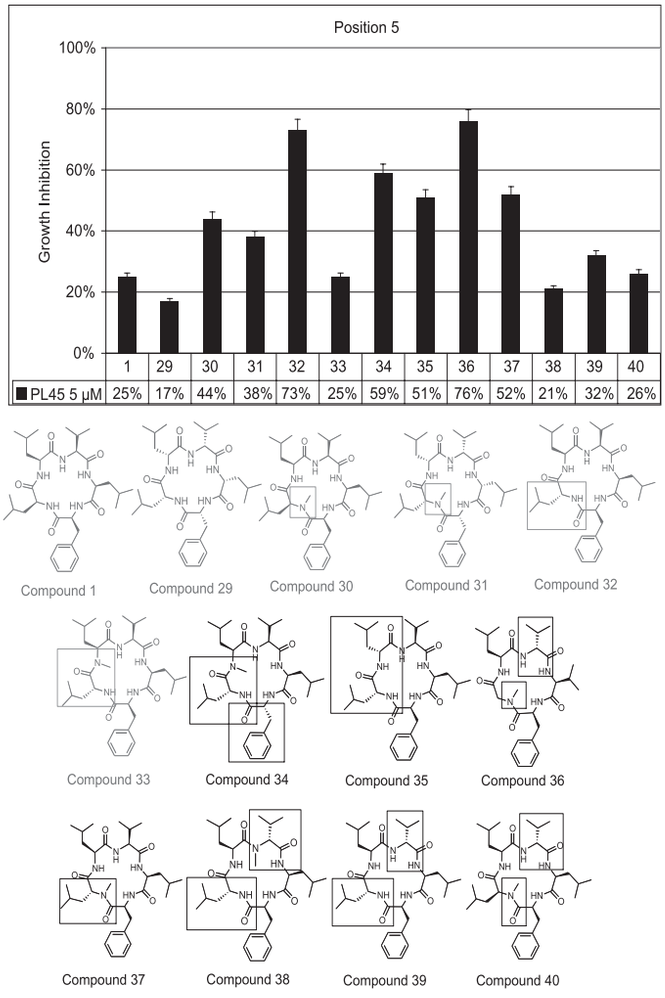

Fig. 8. Compounds with changes to position 5. Grey compounds **1**, **29**, **30**, **31**, **32**, and **33** are first generation compounds, while black compounds **34**, **35**, **36**, **37**, **38**, **39**, and **40** are second-generation. Each data point is an average of three wells run in three assays. Error = ±5%.

sion of that rule. Interestingly, the most potent compound encountered against the PL-45 cell line is compound **36**. This compound has one familiar feature that has been previously identified to be important, which is a *D*-valine at key position **3** [6]. Finally, an important aspect shown by this SAR is that polar compounds, regardless of the positional placement of the polar amino acid, are ineffective: **4**, **15**, **10**, and **23**. Polar groups seem to decrease the hydrophobicity of these macrocycles, thus possibly decreasing its ability to be rapidly absorbed through lipophilic membranes. In support of our findings others have done work and shown that inclusion of a single *N*-methyl, *D*-amino acid, or *N*-methyl *D*-amino acid locks a pentapetide macrocycle into a single conformation, it is presented to the appropriate biological target (s) [14,15,20]. These findings provide an explanation for why compounds **8**, **12**, **20**, **32**, **34**, **36**, and **37** are active. That is, they all contain these individual features. According to Kessler and Marshall the key is positional placement of these features relative to the side chains. Thus, each compound above has unique placement of the sidechains and therefore the inclusion of the *N*-methyl or *D*-aa or *N*-methyl *D*-aa is distinct to lock these side chains into an "active" conformation.

IC_{50} of potent compounds

The IC_{50} values for the eight most potent compounds are shown (Figure 9). Importantly, all eight compounds exhibit very low micro molar IC_{50} values for PL-45. Four compounds, **8**, **12**, **32**, and **36**, show greater than 14 fold more potency than the natural product peptide **1** against this cell line.

The IC_{50} values show the same general trend observed from SAR derived from San A analogs: the importance of a single *N*-methyl, an *N*-methyl *D*-aa, and hydrophobicity. Six out of eight compounds that display potency contain one of the

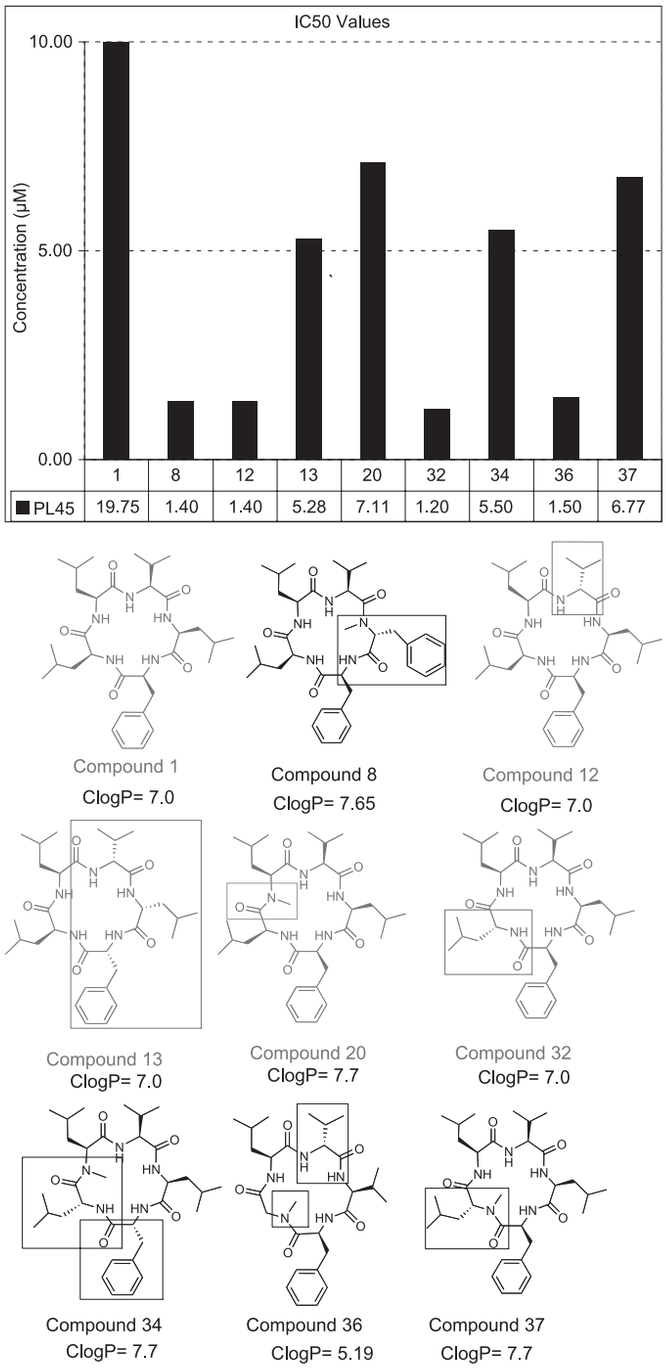

Fig. 9. IC_{50}s of potent compounds. Each data point is an average of the three wells run in three assays at four different concentrations. DMSO was used as the negative control.

3 features: **8**, **12**, **20**, **32**, **36**, and **37**. The other two compounds, **13** and **34**, both contain multiple *D*-aas, where **13** has 3 and **34** has 2 *D*-aas. Thus, these two compounds still follow the same trend as the other 6, but it appears that additional D-aa's are needed in order to lock these side chains into an active conformation for binding to their biological target. It is important to note that of the 8 active compounds reported below, 3 of the 4 most active compounds, **12**, **32**, and **36**, contain a single *D*-aa, where as the other 5 compounds incorporate multiple *D*-aas or an *N*-methyl *D*-aa or an *N*-methyl aa. In summary, the IC_{50}s of these 8 active compounds show that these derivatives are potential lead structures for further therapuetic development, where 4 compounds in particular have specific structural modifications that can be used in future analog synthesis.

Molecular Modeling

Given that compound **8** displays a much higher (25%) growth inhibition value than **9**, compounds **8** vs. **9** were modeled to detail the conformational affect due to the presence of an *N*-methyl amino acid on position 2. In addition, compounds **34** vs. **33** were modeled to detail the conformational fluctuation due to the affect of multiple *D*-aa's, as **9** emulates **8** but includes a *D*-phenylalanine at position 1. These groups were chosen to represent the dynamical picture of the San A derivatives as they are introduced to the protein target.

The molecular modeling study of compounds **8** vs. **9** as well as **34** vs. **33** provided a visual picture of conformational alteration on the peptide backbone due to the addition of *N*-methyl amino acids as well as stereo chemical fluctuation between *L* and *D*-aa's. Computational analysis was conducted using Schrödinger's MacroModel within the Maestro console [1] (Mohamadi, F). Force field-based molecular modeling was exhausted in order to examine conformations at the lowest global minimal energy. The lowest global minimum is taken as a common reference between multiple compounds that do not share similar minimal energy. Detailed conformational searches with strict energy and steric qualifications produced 3,435 independent conformers for compound **8**, 3,017 independent conformers for compound **9**, 7,800 independent conformers for **34** and 8, 329 independent conformers for **33**. All four compounds conformers were individually superimposed on the peptide backbone to represent the average low energy conformation after a pool of redundant conformers was eliminated* (Figure 10).

Comparing compounds **8** and **9** provides evidence that the presence of an *N*-methyl within the macrocycle generates a higher energy structure. The global minimum energy for **8** was shown to be 431.512 kJ mol^{-1} and the global minimum for **9** was 357.014 kJ mol^{-1}. In this scenario, the lowest energy conformation does not necessarily result in the most bioactive conformation. As a result of the evident conformational fluctuation along the peptide backbone in compound **9** this scenario depicts a more stable conformation (as shown in **8**) and produces the more bioactive conformer. The stability of the conformational space is most apparently due to the inclusion of the *N*-methyl amino acid at position two as it is seen not only locking the ring in a stable conformation but limiting the available space for the subsequent side chains to inhibit.

Comparing compounds **34** and **33** provides evidence that the fluctuation between *L* and *D*-aa's does not significantly affect the global minimum energy of the peptide. Compound **34** has a global minimum energy of 371.517 kJ mol^{-1} and the global minimum of **33** was 369,959 kJ mol^{-1}. Compound **34**

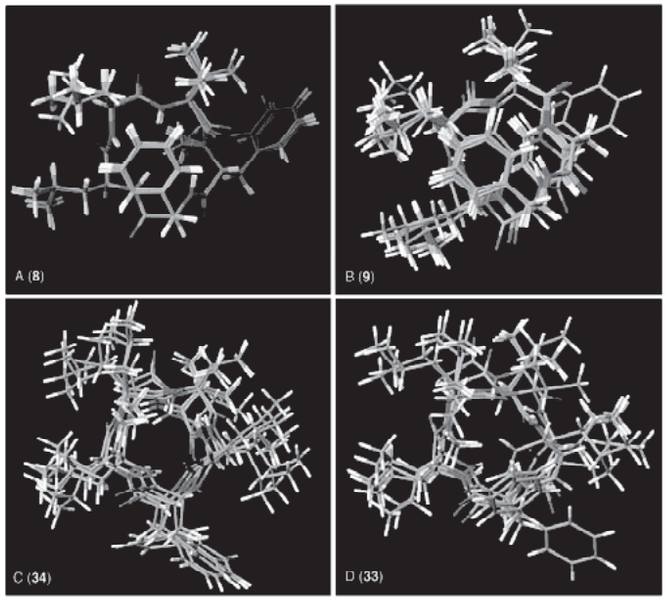

Fig. 10. Computational analyses using Schrödinger's MacroModel within Maestro. Conformational searches were done using the MMFF94 force field and parameters were set with a dielectric constant of 1.0. Compound **8** was calculated to have an average low energy conformation of 431.512 kJ mol^{-1} (A). Compound **9** was calculated to have an average low energy conformation of 357.014 kJ mol^{-1} (B). Compound **34** was calculated to have an average low energy conformation of 369.959 kJ mol^{-1} (C). Compound **33** was calculated to have an average low energy conformation of 371.517 kJ mol^{-1} (D).

is an emulation of **33** with a *D*-phenylalanine at position 1. Conformational fluctuation along the peptide backbone is evident in both compounds **34** and **33**, however the conformation of the phenylalanine at position 1 potentially holds the key to communication with the protein target.

Summary of Molecular Modeling Results

In summary, compounds **8** and **9** were modeled to examine the three-dimensional consequence of the addition of an *N*-methyl amino acid. This comparision demonstrates that an *N*-methyl *D*-aa is key to locking the molecule into this position, whereas simply a *D*-aa at this position does not generate an active conformation. Compounds **33** and **34** were chosen for similar reasons, where their structures only differ by a single *D*-aa. Thus, comparing the lowest energy conformation of the active compound **34** to the much less active **33** we are able to understand the 3-*D* conformation of the active molecule relative to the inactive molecule. Thus, these Force field-based modeling studies are a helpful method for restricting conformation and providing critical analysis of potent 3-D structures.

Annexin V apoptosis detection

Sansalvamide A analogs have been identified as potent apoptotic inducers via G0/G1 cell-cycle arrest [7,8]. Using an Annexin V apoptosis detection assay, compound **8** was analyzed using non-serum deprived cells via flow cytometry for its ability as an apoptotic inducer in the PL-45 cell line. It is important to note that previous efforts in identifying San A analogs as potent apoptotic inducers used serum deprived cells, which is known to induce apoptotic cell death. Four experiments were ran at 3 time points (=15 experiments total): a) cells + 1% DMSO, b) cells + 1% DMSO + 10μ*M* **8**, c) cells + 1% DMSO + 10μ*M* GDA, and d) cells + 1% DMSO + 10μ*M* gemcitabine. Three standards were also ran: Annexin V only, propidium iodide (PI) only, and both Annexin V and PI to mixtures of the cells. The bottom right quadrant represents cells in apoptosis. 1% DMSO was used as the baseline and compared to experiments where compound was added. Annexin V is very sensitive, and even a small fold increase of apoptosis will indicate that our compound is utilizing this mechanism for killing cells. Gemcitabine did not induce apoptosis (i.e. the % apoptosis seen with 10μ*M* gemcitabine was the same as that observed for 1% DMSO), which is consistent with gemcitabine's mechanism of action. GDA induced apoptosis 2 fold over background, compound (**8**) induced apoptosis by >4 fold in PL-45 over DMSO, and as expected, BITC induced apoptosis as well.

Figure 11 shows a total of 100,000 events using Annexin V protein-FITC chromophore conjugates and non-serum deprived PL-45 cells. The upper left corner of the quadrants represent the dead cells, lower left are live cells, upper right are necrotic cells, and lower right are apoptotic cells. Compound **8** shows 4 times more apoptosis at 10μ*M* in PL-45 cells than 1% DMSO alone. Therefore, San A derivative **8**'s ability to kill cells via apoptosis shows the drug is selective in its target. Also, if a compound induces death via an apoptotic pathway, then this molecule will cause fewer toxic side reactions *in-vivo* than if it induced death via an uncontrolled traumatic event (necrosis).

Conclusion

Previous SAR studies in PL-45 [9] include the incorporation of a *D*-phenylalanine or *N*-methyl at position 1, a *D*-valine at 3, and an *N*-methyl or *N*-methyl *D*-leucine at 5. It was con-

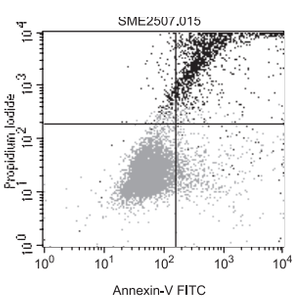

Quadrant Statistics

File: SME2507.015
Sample ID: 10 μM 1.5 hr
Gate: Region 1
Total Events: 100000
Quad Location: 161, 193

Quad	Events	% Gated	X Geo Mean
UL	2266	2.36	107.13
UR	13442	14.00	598.34
LL	75245	78.37	51.97
LR	5060	5.27	482.15

Fig. 11. Annexin V apoptosis detection using Annexin V protein-FITC chromophore conjugates and non-serum deprived PL-45 cells.

cluded that a single feature or position is not responsible for potency, rather as is typical in complex systems, in fact there are several determining factors. Also, it was discussed that the key connection between potency and structure involved constraining the macrocycle into its active conformation. Furthermore, recent publications highlighted that a single *N*-methyl *D*-aa was the central structural component required to maintain a dominant conformation in macrocycles with five amino acids [20,27]. Indeed, the incorporation of an *N*-methyl, combined with a *D*-aa re-affirms this key SAR in the second generation, producing 5 highly potent compounds: **8**, **20**, **34**, **36**, and **37**. Also, a more detailed SAR identified novel key features such as an *N*-methyl containing scaffold with two aromatic Phenylalanines in sequence **8**, and an *N*-methyl in conjugation with two adjacent *D*-aa's (**34**) have been identified and validated using computational analyses. The Schrödinger's MacroModel within the Maestro program has proven to be a useful tool to further identify and characterize possible potent conformers based on the global minimum energies of the lead active scaffolds. Finally, using non-serum deprived cells and an Annexin V detection study has proven that compound **8** displays the ability to induce apoptosis (Figure 11). Compound **8** showed up to 4 times more apoptotic events than DMSO in PL-45, displaying the potential of such macrocyclic analogs as selective apoptotic inducers of cancer cells. In addition to causing apoptosis, these experiments showed that our compounds are cytotoxic rather than cytostatic. We measured the initial percentage of cells with intact members to be 89% and found that after exposure to **8** for 3 h this percentage is only 71%. This is a significant decrease in viable cells, and indicates that our compound is killing cells rather then behaving via a cytostatic mechanism.

Experimental Procedures

Thymidine incorporation/Growth inhibition assay

Proliferation of the PL-45 pancreatic cancer was tested in the presence and absence of the compounds using ^{3}H-thymidine uptake assays. Cells treated with the compounds were compared to DMSO-treated controls for their ability to proliferate as indicated by the incorporation of ^{3}H-thymidine into their DNA. Cells were cultured in 96 well plates at a concentration of 2,500 cells/well. The media was DMEM for PL-45 supplemented with *L*-glutamine, 10% fetal bovine serum and 1% penicillin-streptomycin antibiotic. After incubation for 6 h, the compounds were added. The compounds were dissolved in DMSO at a final concentration of 1% and tested at the concentrations indicated in the manuscript. The DMSO concentration was held constant in all wells at 1%. After the cells had been incubated with the compounds for 56 h, 5mCi ^{3}H-thymidine per well was added and the cells were cultured for an additional 16 h (for the cells to have a total of 72 hr with the drug), at which time the cells were harvested using a PHD cell harvester from Cambridge Technology Incorporated. The samples were then counted in a scintillation counter for 2 m each using ScintiVerse universal scintillation fluid from Fisher. Decreases in ^{3}H-thymidine incorporation, as compared to controls, are an indication that the cells are no longer progressing through the cell cycle or synthesizing DNA, as is shown in the studies presented.

Molecular modeling studies

Computational analysis was conducted using Schrödinger's MacroModel within the Maestro console. Conformational searches using Monte Carlo techniques were done using the MMFF94 force field. The Monte Carlo contribution gives a wide selection of torsional possibilities and assures all possible torsional models are expressed. All energy qualifications are specified to reduce the abundance of redundant conformers. The parameters were set with a dielectric constant of 1.0 in order to dampen the contribution of electrostatics, thus no solvation was selected to remove possibility of over-dampening the electrostatic contribution. The effect of solvent can greatly effect the energy contribution since the electrostatically least stable structures tend to be the most greatly solvated in a polar solvent. The analysis downplays the electrostatic contribution, and focuses on the l searches reflecting the effect of sterics in order to gauge intermolecular effects. The truncated-Newton conjugate-gradient (TNCG) energy minimization was used as an iterative technique to be stopped as soon as the above listed criterion were reached. In order to reduce redundant conformers, we report mixed torsional/low-mode sampling and 30,000 steps of calculation. These variables produced 3,435 independent conformers for compound **8**, 3,017 independent conformers for compound **9**, 8,329 independent conformers for compound **33**, and 7,800 independent conformers for compound **34**. Conformers within specified global minimum energies were superimposed on the peptide backbone to yield an average low energy representation, thus highlighting the available conformational space.

Compound* **8: Compounds within 1.0 kcal mol^{-1} of the global minimum were superimposed to highlight the conformational space obtained for the average lowest energy. Six total compounds were superimposed, ranging from 431.512 kJ mol^{-1} to 435.648 kJ mol-1. The global minimum obtained through the listed variables was 431.512 kJ mol^{-1}. The conformational search produced 3,435 independent conformers. 6 structures within 1.0 kcal mol^{-1} of global minimum were superimposed.

Compound* **9: Compounds within 2.0 kcal mol^{-1} of the global minimum energy were superimposed and shown as a representation of the average low energy conformation. 1 structure was within 1.0 kcal mol^{-1}, thus we chose to depict 2.0 kcal mol^{-1} for it gave 6 structures and a better overall view of the average conformational space. Six total compounds were superimposed ranging from 357.014 kJ mol^{-1} to 364.616 kJ mol^{-1}. The global minimum obtained using the variables listed was 357.014 kJ mol^{-1}. The conformational search produced 3,017 independent conformers.

Compound* **34: Compounds within 1.0 kcal mol^{-1} of the global minimum energy were superimposed and shown as a representation of the average low energy conformation. Five total compounds were superimposed ranging from 371.517 kJ mol^{-1} to 375.688 kJ mol^{-1}. The global minimum obtained using the variables listed was 371.517 kJ mol^{-1}. The conformational search produced 7,800 independent conformers.

Compound* **33: Compounds within 0.5 kcal mol^{-1} of the global minimum energy were superimposed and shown as a representation of the average low energy conformation. Given that there were 9 structures within 1.0 kcal mol^{-1} it was chosen to depict 0.5 kcal mol^{-1} for it gave 4 structures and evidently eliminated multiple redundant conformers. Four total compounds were superimposed ranging from 369.959 kJ mol^{-1} to 371.387 kJ mol^{-1}. The global minimum obtained using the variables listed was 369.959 kJ mol^{-1}. The conformational search produced 8,329 independent conformers.

Annexin V apoptosis detection

In preparation for apoptosis detection, PL-45 cells were maintained in a sub confluent monolayer at 37°C in a humidified incubator with 5% CO_2. They were propagated with DMEM medium and supplemented with L-glutamine, 10% fetal bovine serum and 1% penicillin-streptomycin. For the assay the respective cells were plated in 6 well plates each containing 500,000 cells and 3 mL of DMEM supplemented medium. The plates were allowed to incubate for 24 h to allow the cells to fully attach to adherent plate(s). After 24 h of incubation each well was inoculated with a 10 μ*M* concentration of compound **8** in 1% DMSO at 37°C for 1.5 h. A control of 1% DMSO was also made to eliminate background apoptosis readings from DMSO alone. After plates were incubated with drug the medium was aspirated off and the cells were washed over with phosphate buffered saline. The cells were then trypsainized to detachment and re-suspended with 3 mL fresh medium into a 15 mL conical tube. The cells were pelleted and re-suspended in 1X binding buffer. The suspension was then incubated with PI and Annexin V conjugated to FITC for 15 m and read via flow cytometry.

Synthesis:

General peptide synthesis

All peptide coupling reactions were carried out under argon with dry solvent, using methylene chloride for dipeptide and tripeptide couplings and acetonitrile for pentapeptide couplings. The amine (1.1 equiv) and acid (1 equiv) were weighed into a dry flask along with 4 equiv of DIPEA and 1.1 equiv of TBTU.* Anhydrous methylene chloride was added to generate a 0.1*M* solution. The solution was stirred at room temperature and reactions were monitored by TLC. Reactions were run for 1 h before checking via TLC. If reaction was not complete an additional 0.25 equiv of HATU and TBTU were added. If reaction was complete then work-up was done by washing with saturated ammonium chloride. (Note: if acetonitrile was used for the reaction, methylene chloride was added to reaction upon workup and the resulting solution was washed with ammonium chloride). After back extraction of aqueous layers with methylene chloride, organic layers were combined, dried over sodium sulfate, filtered and concentrated. Flash chromatography using a gradient of ethyl actetate-hexane gave our desired peptide.

* Some coupling reactions would not go to completion using only TBTU and therefore ~0.25 equiv of HATU, and/or DEPBT were used. In a few cases up to 1.1 equiv of all three coupling reagents were used.

General Amine deprotection

Amines were deprotected using 20% TFA in methylene chloride (0.1*M*) with 2 equiv of anisole. The reactions were monitored by TLC, where the TLC sample was first worked up in a mini-workup using DI water and methylene chloride to remove TFA. Reactions were allowed to run for 1-2 h and then concentrated in vacuo.

General Acid deprotection

Acids were deprotected using ~4 equiv of lithium hydroxide (or until pH = ~11) in methanol (0.1 *M*). The peptide was placed in a flask, along with lithium hydroxide and methanol, and stirred overnight. Within 12 h the acid was usually deprotected. Work-up of reactions involved the acidification of reaction solution using HCl to pH = 1. The aqueous solution was extracted three times with methylene chloride, and the combined organic layer was dried, filtered and concentrated in vacuo.

Macrocyclization procedure (in situ)

All pentapeptides were acid and amine deprotected using concentrated HCl (8 drops per 0.3mmols of linear pentapeptide) in THF (0.05*M*). Anisole (2 equiv) was added to the reaction and the reaction was stirred at room temperature. The reaction typically took 4 d, but TLC and LCMS were used to monitor the reaction every 12 h. LCMS data typically indicated the reaction was ~50% complete after the first day. Addition of four drops of concentrated HCl per 0.3 mmol of pentapeptide, stirring at RT overnight and checking the reaction via LCMS usually showed ~75% completion. On the fourth day verification of the presence of the free amine and free acid and disappearance of the starting linear protected pentapeptide permitted workup. The reaction was concentrated in vacuo and the crude, dry, double deprotected peptide (free acid and free amine) was dissolved in a minimum solution of THF: acetonitrile: methylene chloride (2:2:1 ratio). Three coupling agents (DEPBT, HATU, and TBTU) were used at ~0.5 to 0.75 equiv each. These coupling agents were dissolved in a calculated volume of dry 40% THF, 40% acetonitrile, and 20% methylene chloride that would give a 0.004 *M* overall solution when included in the volume used for the deprotected peptide. The coupling

agents were then added to the deprotected peptide solution. DIPEA (6 equiv or more in order to neutralize the pH) were then added to the reaction. The coupling agents are typically not very soluble in acetonitrile, which is why a combination of solvents is used.

After 1 h, TLC and LCMS (where the LCMS sample was worked up prior to injection) indicated that a product spot was developing. The comparison Rf value in the product spot on TLC was the protected linear pentapeptide. The reactions were always complete after 2 h, and monitoring the starting material deprotected pentapeptide via LCMS was the easiest method of determining completion. Upon completion, the reaction was worked up by washing with saturated ammonium chloride. After back extraction of aqueous layers with large quantities of methylene chloride, the organic layers were combined, dried, filtered and concentrated. All macrocycles were purified by initially running a crude plug of compound using an ethyl acetate/hexane gradient on silica gel, then running a column on the isolated product. Finally, when necessary reverse phase HPLC was used for additional purification using a gradient of acetonitrile and DI water with 0.1% TFA.

Acknowledgements

We thank San Diego State University for financial support. We thank the Howell Foundation for support of R.A.R and R.C.V. We thank NIH (T90DK07015) for support of W.S.D. We thank the MHIRT program for their support of R.A.R.

Supporting information available

A table that includes the description of all changes made to compound structures in text format is included in the supporting information. IC_{50} data curves are supplied in the supplementary material. This material is available free of charge on the Internet.

References

1. (a) Burris, H. A.; Moore, M. J.; Andersen, J.; Greem, M. R.; Rothenberg, M. I.; Modiano, M. R.; Cripps, M. C.; Portenoy, R. K.; Sotorniolo, A. M.; Tarassaoff, P.; Nelson, R.; Dorr, F. A.; Stephens, C. D.; vonHoff, D. *J. Clin. Oncol.* **1997**, *15*, 2403-2413. (b); Fennelly, D.; Kelsen, D. P. Hepatogastroenterology 1996, 43, 356-362. (c); Schnall, S. F.; Mcacdonald, J. S. *Semin. Oncol.* **1996**, *23*, 220-228.
2. (a) Cueto, M.; Jensen, P. R.; Fenical, W. *Phytochemistry* **2000**, *55*, 223-226. (b) Hwang, Y.; Rowley, D.; Rhodes, D.; Gertsch, J.; Fenical, W.; Bushman, F. *Mol. Pharmacol.* **1999**, *55*, 1049-1053.
3. Belofsky, G. N.; Jensen, P. R.; Fenical, W. *Tetrahedron Lett.* **1999**, *40*, 2913-2916.
4. Liu, S.; Gu, W.; D., L.; Ding, X.-Z.; Ujiki, M.; Adrian, T. E.; Soff, G. A.; Silverman, R. B. *J. Med. Chem.* **2005**, *48*, 3630-3638.
5. Ujiki, M.; Milam, B.; Ding, X.-Z.; Roginsky, A. B.; Salabat, M. R.; Talamonti, M. S.; Bell, R. H.; Gu, W.; Silverman, R. B.; Adrian, T. E. *Biochem. Biophys. Res. Commun.* **2006**, *340*, 1224-1228.
6. Pan, P. S.; McGuire, K.; McAlpine, S. R. *Bioorg. Med. Chem. Lett.* **2007**, *17*, 5072-5077.
7. Otrubova, K.; Styers, T. J.; Pan, P.-S.; Rodriguez, R.; McGuire, K. L.; McAlpine, S. R. *Chem. Commun.* **2006**, 1033-1034.
8. Styers, T. J.; Kekec, A.; Rodriguez, R. A.; Brown, J. D.; Cajica, J.; Pan, P.-S.; Parry, E.; Carroll, C. L.; Medina, I.; Corral, R.; Lapera, S.; Otrubova, K.; Pan, C.-M.; McGuire, K. L.; McAlpine, S. R. *Bioorg. Med. Chem.* **2006**, *14*, 5625-5631.
9. Carroll, C. L.; Johnston, J. V. C.; Kekec, A.; Brown, J. D.; Parry, E.; Cajica, J.; Medina, I.; Cook, K. M.; Corral, R.; Pan, P.-S.; McAlpine, S. R. *Org. Lett.* **2005**, *7*, 3481-3484.
10. (a) Otrubova, K.; Lushington, G. H.; Vander Velde, D.; McGuire, K.; McAlpine, S. R. J. Med. Chem., in press. (b) Otrubova, K.; McGuire, K. L.; McAlpine, S. R. *J. Med. Chem.* **2007**, *50*, 1999-2002.
11. (a) Reed, J. C.; Pellecchia, M. *Blood* **2005**, *106*, 408-418. (b) Green, D. R.; Kroemer, G. *Science* **2004**, *305*, 626-629. (c) Guimaraes, C. A.; Linden, R. *Eur. J. Biochem.* **2004**, *271*, 1638-1650.
12. Hasan, N. M.; Adams, G. E.; Joiner, M. C. *Int. J. Cancer* **1999**, *80*, 400-405.
13 The ClogP values were calculated using an algorithm. The logP value of a compound, which is the logarithm of its partition coefficient between n-octanol and water log(coctanol/cwater), is a well established measure of the compound's hydrophilicity. Low hydrophilicities and therefore high logP values cause poor absorption or permeation. It has been shown for compounds to have a reasonable probability of being well absorbt their logP value must not be greater than 5.0. The distribution of calculated logP values of more than 3000 drugs on the market underlines this fact.
14. Chatterjee, J.; Mierke, D. F.; Kessler, H. *J. Am. Chem. Soc.* **2006**, *128*, 15164-15172.
15. Heller, M.; Sukopp, M.; Tsomaia, N.; John, M.; Mierke, D. F.; Reif, B.; Kessler, H. *J. Am. Chem. Soc.* **2006**, *128*, 13806-13814.
16. Styers, T. J.; Rodriguez, R. A.; Pan, P.-S.; McAlpine, S. R. *Tetrahedron Lett.* **2006**, *47*, 515-517.
17. Dipeptide and tripeptide structures were confirmed using 1H NMR. All linear pentapeptides were confirmed using LCMS and 1H NMR. (Note: ^{1}H NMR were taken for cyclized peptides, but due to their complexity, they were not seen as the primary confirmation for cyclized compounds). See supplementary data for spectra.
18. Unpublished results from the Guy lab at Department of Chemical Biology and Therapeutics, St Jude Children's Research Hospital, Memphis, TN 38103, and published results from our lab show that the use of several coupling reagents facilitates formation of the peptide bond in high-yields.
19. (a) Bolla, M. L.; Azevedo, E. V.; Smith, J. M.; Taylor, R. E.; Ranjit, D. K.; Segall, A. M.; McAlpine, S. R. Org. Lett. 2003, 5, 109-112. (b) Liotta, L. A.; Medina, I.; Robinson, J. L.; Carroll, C. L.; Pan, P.-S.; Corral, R.; Johnston, J. V. C.; Cook, K. M.; Curtis, F. A.; Sharples, G. J.; McAlpine, S. R. *Tetrahedron Lett.* **2004**, *45*, 8447-8450.
20. Zhang, X.; Nikiforovich, G. V.; Marshall, G. R. *J. Med. Chem.* **2007**, *50*, 2921-2925.